Tomato spotted wilt virus glycoproteins induce the formation of endoplasmic reticulum- and Golgi-derived pleomorphic membrane structures in plant cells

Daniela Ribeiro,[1] Ombretta Foresti,[2] Jurgen Denecke,[2] Joan Wellink,[3] Rob Goldbach[1] and Richard Kormelink[1]

[1]Wageningen University, Laboratory of Virology, Binnenhaven 11, 6709 PD Wageningen, The Netherlands

[2]University of Leeds, Centre for Plant Sciences, Clarendon Way, Leeds LS2 9JT, UK

[3]Wageningen University, Laboratory of Molecular Biology, Dreijenlaan 3, 6703 HA Wageningen, The Netherlands

Correspondence
Richard Kormelink
richard.kormelink@wur.nl

Tomato spotted wilt virus (TSWV) particles are spherical and enveloped, an uncommon feature among plant infecting viruses. Previous studies have shown that virus particle formation involves the enwrapment of ribonucleoproteins with viral glycoprotein containing Golgi stacks. In this study, the localization and behaviour of the viral glycoproteins Gn and Gc were analysed, upon transient expression in plant protoplasts. When separately expressed, Gc was solely observed in the endoplasmic reticulum (ER), whereas Gn was found both within the ER and Golgi membranes. Upon co-expression, both glycoproteins were found at ER-export sites and ultimately at the Golgi complex, confirming the ability of Gn to rescue Gc from the ER, possibly due to heterodimerization. Interestingly, both Gc and Gn were shown to induce the deformation of ER and Golgi membranes, respectively, also observed upon co-expression of the two glycoproteins. The behaviour of both glycoproteins within the plant cell and the phenomenon of membrane deformation are discussed in light of the natural process of viral infection.

INTRODUCTION

Tomato spotted wilt virus (TSWV) is the type species of the genus *Tospovirus* within the family (of primarily arthropod-borne) *Bunyaviridae*. Unlike most members of this family, tospoviruses are able to infect plants, rather than animals, and are transmitted in a propagative manner by thrips species (order, Thysanoptera; family, Thripidae) (Elliott, 1990; Goldbach & Peters, 1996). TSWV particles have a lipid envelope containing the virally encoded glycoproteins Gn and Gc (n and c refer to the N- and C-terminal topology, respectively, within the precursor protein), a rather unique feature among plant viruses, reflecting the requirement for uptake and replication of the virus in its insect vector (Wijkamp *et al.*, 1993). Virus particles harbour a tripartite negative/ambisense RNA genome that, in association with the nucleocapsid protein (N) and the viral RNA-dependent RNA polymerase (L), forms infectious ribonucleoproteins (RNPs) (Goldbach & Peters, 1996; Mohamed *et al.*, 1973).

For the animal infecting bunyaviruses, particle assembly involves budding of RNPs into the enlarged lumen of glycoprotein containing Golgi, leading to the formation of single-enveloped virus particles (SEVs), which are then secreted from the cells (Booth *et al.*, 1991; Elliott, 1990, 1996; Gahmberg *et al.*, 1986; Griffiths & Rottier, 1992; Jantti *et al.*, 1997; Kuismanen *et al.*, 1982; Lyons & Heyduk, 1973; Petterson & Melin, 1996; Rwambo *et al.*, 1996; Salanueva *et al.*, 2003; Smith & Pifat, 1982). In contrast, during TSWV infection of plant cells, mature virus particles arise as a result of wrapping of the entire Golgi cisternae around RNPs (Kikkert *et al.*, 1997, 1999, 2001; Kitajima *et al.*, 1992; Petterson & Melin, 1996). As a result, double-enveloped virus particles (DEVs) are formed that fuse with each other and with endoplasmic reticulum (ER)-derived membranes leading to the formation of mature SEVs clustered inside large vesicles within the cytoplasm. There, the virus is retained prior to uptake by the insect vector upon feeding (Kikkert *et al.*, 1999). However, upon infection of thrips (salivary gland) cells, mature TSWV particles do not accumulate inside the cells. Instead, they are secreted in resemblance to what is observed during the maturation pathway of animal infecting bunyaviruses (Whitfield *et al.*, 2005).

The final fate of mature TSWV particles in plant and insect cells is clearly distinct and likely reflects adaptations of this virus to either cell type. Based on sequence similarities, it has been hypothesized that TSWV shares a common ancestor with members of the genus *Orthobunyavirus*, from which it evolved upon adaptation to plant cells, while still retaining the capability to replicate and form virus particles in thrips (animal) cells (Goldbach & Peters, 1996).

As the viral glycoproteins localize, guide and potentiate the process of enveloped virus assembly, it becomes important to study their individual and combined behaviour upon expression in both animal and plant cells, in order to identify domains within the glycoproteins responsible for the critical differences between the intracellular targeting in either cell system. Initial studies revealed that, in mammalian cells (Kikkert *et al.*, 2001), the TSWV glycoproteins exhibit a similar trafficking behaviour to those from the animal infecting bunyaviruses (Andersson *et al.*, 1997; Elliott, 1996; Matsuoka *et al.*, 1996; Rönnholm, 1992).

In this study, a detailed analysis of the localization and behaviour of the TSWV glycoproteins within the plant cell presented new insights, crucial to further unravel and understand the entire virus particle maturation process in its natural host.

METHODS

Plasmid construction and organelle markers.

The pMON999 vector (containing a 35S-driven promoter) was used for cloning and expression of the fluorophore-fused and non-fused TSWV proteins. The previously established pSFV plasmid containing the glycoprotein precursor (GP) (Kikkert *et al.*, 2001), as well as the Gc–yellow fluorescent protein (YFP) and Gn–YFP (Snippe *et al.*, 2007), were subjected to a restriction enzyme digestion with *Bam*HI, which resulted in the isolation of a cloning cassette containing the respective fused and non-fused glycoproteins. The multiple cloning site *Bam*HI was used to insert these cassettes into the (previously digested and dephosphorylated) pMON999 vector.

For fusion of the YFP to the C terminus of the glycoprotein precursor, pMONGP was digested with *Nhe*I (single restriction site within Gc) and *Bam*HI, allowing the isolation of a cassette containing part of the glycoprotein precursor cleaved at 500 nt from the 5′ end. The digestion with *Nhe*I and *Bam*HI was also performed on pSFVGc–YFP, allowing the isolation of a cassette containing part of Gc–YFP, cleaved at 1765 nt from its 3′ end. A three-point ligation was performed between the two previously mentioned cassettes and the *Bam*HI digested pMON999, resulting in the construction of pMONGP–YFP.

A plant expression vector containing cyan fluorescent protein (CFP) fused to the C terminus of Gc (p2GW7.0Gc–CFP) was obtained using the Gateway system (Invitrogen), following the manufacturer's instructions. The primers GcFwdGW (5′-GGGGACAAGTTTGTACAAAAAAGCAGGCTGGATGAGTGTACTAAAGTCTGCATTTC-3′) and CFPRvsGW (5′-GGGGACCACTTTGTACAAGAAAGCTGGGTGTTACTTGTACAGCTCGTCC-3′) were used to PCR amplify Gc–CFP from the pSFVGc–CFP construct (Snippe *et al.*, 2007). The PCR fragment was introduced into pDonr207 by BP recombination and subsequently into the p2GW7.0 (Karimi *et al.*, 2002) destination vector by LR recombination.

The fluorescent proteins used in this study for fusion to the viral glycoproteins were a pH-insensitive form of YFP, CFP and mGFP5 (Haseloff *et al.*, 1997). The spectral properties of mGFP5 allow efficient spectral separation from YFP (Brandizzi *et al.*, 2002).

In these experiments we made use of the green fluorescent protein (GFP)–HDEL ER marker (Carette *et al.*, 2000), the ST–GFP Golgi marker (Boevink *et al.*, 1998), the YFP–Sec24 ER-export site (ERES) marker (Stefano *et al.*, 2006) and the prevacuolar compartment marker (PVC), GFP–BP80 (da Silva *et al.*, 2005).

Plant material and transient expression.

Tobacco plants (*Nicotiana tabacum* cv Petit Havana) (Maliga *et al.*, 1973) were grown in Murashige and Skoog medium (Murashige & Skoog, 1962) with 2% sucrose, in controlled sterile conditions at 25 °C with a 16 h period of light per day. Tobacco leaf protoplast preparation and transfection were performed as described by Denecke & Vitale (1995), with some minor modifications. In short, leaves of fully grown plants were pierced and digested overnight in TEX buffer (B5 salts, 500 mg MES l^{-1}, 750 mg $CaCl_2.2H_2O$ l^{-1}, 250 mg NH_4NO_3 l^{-1}, 0.4 M sucrose, pH 5.7) containing 0.2% Macerozyme and 0.4% cellulase. Protoplasts were recovered by filtration and washed by multiple centrifugations for 15 min at 100 **g** (room temperature) with electroporation buffer (EB) (0.4 M sucrose, 2.4 g HEPES l^{-1}, 6 g KCl l^{-1}, 600 mg $CaCl_2.2H_2O$ l^{-1}, pH 7.2). Healthy living protoplasts were recovered and resuspended in the proper EB volume (500 µl per electroporation experiment). A volume of 100 µl of plasmids in EB (applied plasmid concentrations depended upon experiment: 30 µg of each construct for co-transfections and 60 µg of the construct when singly transfected) was added to 500 µl of protoplast suspension and this mixture was subjected to electroporation (160V, 925 F, $\infty\Omega$) in 4 mm cuvettes using a Bio-Rad X-cell electroporator. After 10 min of recovery, the protoplasts were incubated in 2 ml TEX buffer in the dark (the incubation times differed per experiment, ranging between 24 and 48 h, as mentioned in the figure legends).

N. tabacum plants stably expressing the ST–GFP Golgi marker (kindly provided by Professor Chris Hawes, School of Life Sciences, Oxford Brookes University, UK) were grown under the previously described conditions and the analyses were conducted in protoplasts isolated and transfected according to the previously described methodology.

Sampling and imaging.

Post-transfection (p.t.) (24–48 h), the living protoplasts were isolated by centrifugation and confocal images were obtained using an inverted Zeiss 510 Laser Scanning Microscope and a ×40 oil or ×63 oil and water immersion objective.

For the imaging of the single expression of YFP-fused viral proteins, excitation lines of an argon ion laser of 488 nm were used with a 505/530 nm bandpass filter in the single-track facility of the microscope. For the imaging of the co-expressing YFP-fused and the GFP-fused proteins (as well as for the imaging of the co-expressing CFP- and YFP-fused proteins), excitation lines of an argon ion laser of 458 nm for GFP and 514 nm for YFP were alternately used with line switching using the multi-track facility of the microscope. Fluorescence was detected using a 458/514 nm dichroic beam splitter and a 470/500 and 535/590 nm bandpass filter for GFP and YFP, respectively. Appropriate controls were

performed to exclude possible crosstalk and energy transfer between fluorochromes. For the simultaneous imaging of YFP and tetramethyl rhodamine iso-thiocyanate (TRITC), excitation lines of an argon ion laser of 488 nm for YFP and 543 nm for TRITC were alternately used with line switching using the multi-track facility of the microscope and fluorescence was detected using a 488/543 nm dichroic beam splitter and the filters BP 505/530 and LP 560 nm for YFP and TRITC, respectively.

Indirect fluorescence analysis.

Intact protoplasts were selected as previously described and carefully placed on a microscope slide coated with 0.05% poly L-lysine. Approximately 5 min after, the slides were submerged in 96% ethanol where the fixation occurred for about 20 min. After a 20 min wash in PBS, the protoplasts were blocked with 5% BSA in PBS for 45 min. The cells were subsequently incubated for 1 h in a 1:1000 dilution of the polyclonal antibody against Gc (raised in rabbit) (Kikkert *et al.*, 1997) in 1% BSA in PBS. Three washing steps of 20 min in PBS preceded 1 h incubation in the dark, in a 1:100 dilution of the secondary antibody (swine anti-rabbit conjugated with TRITC) in 1% BSA in PBS. The cells were again washed with PBS in three steps of 20 min, always in the dark. The entire experiment was performed at room temperature. Two drops of citifluor were added to the slides, prior to their examination under an inverted Zeiss 510 Laser Scanning Microscope.

RESULTS

TSWV Gn and Gc glycoproteins show different localization patterns and are able to induce the formation of pleomorphic membrane structures in protoplasts

To study the properties and behaviour of the TSWV glycoproteins in plant cells, both proteins, Gn and Gc, were transiently expressed in protoplasts, either individually or from their common precursor. Separate constructs were made (Fig. 1) and cloned into pMON999 for 35S-driven transient expression in plant cells. Both Gn and Gc were fused to YFP at their C terminus (Fig. 1) to allow immediate monitoring. YFP was also fused to the C terminus of the glycoprotein precursor gene (GP) (Fig. 1), for easy monitoring of Gc in the presence of Gn, as the *in situ* processing of such precursor fusion protein leads to mature Gc–YFP and Gn.

N. tabacum protoplasts were transfected with the individual constructs and analysed by confocal microscopy. These analyses revealed the presence of Gn–YFP in a reticular pattern, indicative of ER-localization, at earlier time points (until 24 h) p.t. (Fig. 2a). At 48 h p.t. (and later), the reticular signal was rarely observed and Gn–YFP was mainly localized in different globular structures (Fig. 2b). Surprisingly, in about 25% of the cells Gn was also found in non-dense pleomorphic structures (Fig. 2c and Fig. 3), mostly circular (Fig. 2c and Fig. 3e–h), although in some cases different shapes were observed (Fig. 3a–d). These structures varied in size, ranging from 0.5 to 4 µm, and in some cases appeared 'open' at one side (Fig. 3g, arrow).

Single expression of Gc–YFP showed a clear reticular localization pattern (Fig. 2d), even after 48 h p.t. Surprisingly, in about 10% of the cells, Gc also localized in pleomorphic membrane structures (Fig. 2e) somewhat similar in appearance to those observed upon expression of Gn–YFP. During several independent experiments more of these structures were discerned, some of these being exceptionally large in size, with a 'diameter' of up to 4 µm.

When both glycoproteins were co-expressed from their common precursor gene fused at the C terminus with YFP (GP–YFP, Fig. 1), monitoring of Gc (i.e. Gc–YFP processed from the precursor) showed that this protein accumulated in small globular structures localized all over the cell (Fig. 2f), a quite distinct pattern from the one observed earlier for Gc–YFP upon single expression (Fig. 2d and e). To analyse whether Gn co-localized with Gc–YFP in these structures, protoplasts were transfected with GP–YFP and prepared for immunolocalization analysis using antibodies directed against Gn. As expected, both glycoproteins co-localized in these structures (results not shown). Furthermore, the

presence of Gn greatly boosted the detection level of Gc (based on the percentage of cells in which the glycoprotein could be observed) to about fivefold.

Fusion of YFP at the C-terminal side of the glycoproteins has recently been shown not to influence their intracellular localization pattern in mammalian cells (Snippe *et al.*, 2007). To verify that, similarly, this fusion did not affect their behaviour in plant cells, protoplasts were transfected with non-fused glycoprotein constructs and analysed by indirect immunolocalization. The non-fused glycoproteins localized similarly to those containing a YFP fusion (data not shown), indicating that the fluorophore fusions did not alter the behaviour of the glycoproteins *in planta*.

Gn localizes to ER, Golgi and Golgi-derived pleomorphic membrane structures

To determine the localization of Gn as well as the origin of the globular/pleomorphic structures, co-expression analyses were performed using ER- and Golgi-specific markers. When protoplasts were co-transfected with Gn–YFP and GFP–HDEL (ER marker) the reticular Gn pattern observed at early times p.t. completely co-localized with this organelle marker (Fig. 4a–c). Protoplasts from plants stably transformed with ST–GFP were similarly transfected with Gn–YFP and revealed that, at later times p.t., Gn co-localized with the Golgi marker. This co-localization was not only observed when Gn localized at the small globular structures (Fig. 4d–f), but also when it localized in the pleomorphic non-dense structures (Fig. 4g–i). These results suggest that Gn, once localized at the Golgi membranes, is able to induce their deformation into pseudo-circular and pleomorphic structures.

Gc is retained in ER and ER-derived pleomorphic membrane structures

To confirm its putative ER localization, Gc–YFP was co-expressed with the GFP–HDEL ER marker. Confocal fluorescence analysis of protoplasts transfected with both constructs revealed a clear co-localization (Fig. 5a–c), which was not restricted to Gc localizing in a reticular pattern, but also when localizing in pleomorphic membrane structures (Fig. 5a–c, arrows).

When protoplasts from tobacco plants stably transformed with ST–GFP were transfected with Gc–YFP, no co-localization between Gc and this Golgi marker (Fig. 5d–f) was observed, even at longer p.t. times (results not shown).

These analyses altogether suggested that Gc is arrested in the ER where it is, similarly to Gn in the Golgi complex, able to modify the morphology of the membranes into pseudo-circular/pleomorphic structures.

Gn is able to redirect Gc from the ER to ERES and subsequently to the Golgi complex

To identify the localization and trafficking of the glycoproteins when expressed from their common precursor gene, GP–YFP was co-expressed with the GFP–HDEL ER marker. The earlier described globular structures containing both glycoproteins (Fig. 2f) did not co-localize with this ER marker (Fig. 6a–c).

Since individually expressed Gn was found to localize in Golgi membranes, and previous studies identified the Golgi complex as the viral assembly locus (Kikkert *et al.*, 1999), Golgi localization of Gc and Gn expressed from their precursor gene was analysed. To this end, protoplasts from plants stably transformed with the ST–GFP Golgi marker were transfected with GP–YFP. Some of the Gc–YFP processed from the precursor and localizing in globular structures co-localized with the Golgi marker (Fig. 6d and f, arrows), but, surprisingly, some clearly did not (Fig. 6d and f, squares) (about 80% of the expressing cells contained, on average, 40% of non-co-localizing structures). To analyse whether part of the glycoproteins would still be retained in specific domains of the ER, non-fluorophore-fused GP was co-expressed with the YFP–Sec24 ERES marker. After 24–48 h, protoplasts were harvested and subjected to immunolocalization with a primary antibody specific for Gc and a secondary antibody fused to TRITC. The results showed (Fig. 6g–i) that part of the glycoproteins indeed co-localized with the ERES marker [whose localization pattern was similar to the one described by Stefano *et al.* (2006)], which allowed us to conclude that Gn is able to induce concentration of Gc at ERES from where they co-migrate, most likely as a heterodimer, to the Golgi complex. To exclude that some of the (non-Golgi) glycoproteins would be present at the PVC, co-expression studies were performed with the GFP–BP80 PVC marker and, as expected, no co-localization was observed (results not shown).

When co-expressed from the common precursor gene, the glycoproteins did not seem to induce the formation of pleomorphic/circular membrane structures. However, it could not be excluded that the observed small, dense-like globular structures (up to 1 µm) may have hollow characteristics that could not be discerned as such due to the microscope resolution. Furthermore, the migration to the Golgi complex of both glycoproteins when expressed from the common precursor gene generally proceeds very quickly, when compared with the single expressions or with the co-expression from separate constructs (results not shown). To test whether the formation of these pleomorphic/circular membrane structures could be visualized upon the kinetically slower co-expression of the glycoproteins from separate constructs, CFP was fused to the C terminus of Gc (Gc–CFP, Fig. 1). Confocal microscopy analysis of protoplasts transfected with Gn–YFP and Gc–

CFP revealed (in about 60% of the expressing cells) the co-localization of the glycoproteins at globular structures, similar to those previously observed upon GP–YFP expression, as well as at the ER (results not shown). Furthermore in the remaining 40% of the expressing cells, the glycoproteins were also found to co-localize at pleomorphic/circular structures (Fig. 6j–l). Altogether these results demonstrate that the pseudo-circular and pleomorphic membrane structures can be induced by any of the glycoproteins, either when singly or co-expressed.

DISCUSSION

In this study we have, for the first time, successfully expressed the TSWV glycoproteins in plant cells without the complicated background of a full infection and, using fluorescence microscopy techniques, described their intracellular localization and behaviour *in vivo*. The data obtained demonstrate that both Gc and Gn glycoproteins, either when co-expressed from separate constructs or from their common precursor gene, are able to reach and retain at the Golgi complex. During this process Gn is able to rescue Gc from the ER, directing it to the Golgi, most likely involving heterodimerization. Upon individual expression, Gn and Gc behave differently, i.e. Gc remains arrested in the ER, whereas Gn is able to leave this organelle and target the Golgi complex, although less efficiently than upon co-expression with Gc. These results confirm the earlier observed properties of the viral glycoproteins upon expression in mammalian cells (Kikkert *et al.*, 2001). Furthermore, they support the idea that, similar to what has been reported for several animal infecting bunyaviruses (Andersson *et al.*, 1997; Elliott, 1996; Matsuoka *et al.*, 1996; Rönnholm, 1992), the combined glycoproteins contain all the information required for their transport and retention in the Golgi complex. Also for TSWV, the glycoproteins seem to guide the process of virus particle assembly.

Surprisingly, our analyses have additionally shown that both glycoproteins, either singly or co-expressed, are capable of causing membrane deformation, inducing the formation of pleomorphic, mostly circular, membrane structures. In case of individual Gc expression these structures were shown to derive from ER, whereas the ones induced by Gn were derived from the Golgi. These hollow structures were apparently absent upon expression of both glycoproteins from their common precursor. However, upon co-expression from separate constructs, these large Gn and Gc containing membrane structures were again observed. Hence, it is possible that the small, dense-like globular structures containing both glycoproteins expressed from the precursor gene, may represent smaller similar structures, whose hollow characteristics could not be discerned due to the limited resolution of the microscope. The same may also apply for the small Golgi-derived globular structures where Gn localizes upon single expression.

Confocal Z-stack analysis showed that, in some cases, these circular membrane structures did not seem to be completely closed. Whether this observation points towards the presence of a heterogeneous pool of membrane structures remains an interesting question to be tackled by using 3D-tomography.

Modification of endomembranes has been reported previously [(Kikkert *et al.*, 1999; Fig. 7)] upon a natural TSWV infection of plants cells. In those studies, electron microscopy

analysis revealed that these modifications, referred to as paired parallel membranes were always restricted to Golgi membranes and ranged in size between 100 and 300 nm. The pseudo-circular and pleomorphic membrane structures observed in the present study ranged in size from 1 to 4 μm, whereas the small globular structures, in which no surrounding membrane could be discerned, ranged from 200 to 500 nm. A possible justification for the large size of these observed membrane structures may lie in induced membrane proliferation, due to the artificial accumulation of high amounts of glycoproteins at these membranes. This accumulation may also result in the enwrapment of an entire Golgi stack around the RNP, and not only a small proportion of the membrane, as suggested to occur during a natural infection (Kikkert *et al.*, 1999). This membrane proliferation may also reflect (on a larger scale) a naturally occurring phenomenon essential for virus assembly, as has been demonstrated for other plant and animal infecting viruses (Barco & Carrasco, 1995; Carette *et al.*, 2002).

Although speculative, it is tempting to hypothesize that the large membrane structures may also arise as a result of membrane fusion of smaller membrane structures. Supporting data comes from studies on TSWV-infected plant cells where, at a certain stage of the infection cycle, newly formed DEVs (Kikkert *et al.*, 1999; Kitajima *et al.*, 1992) fuse with each other and with ER-derived membranes, giving rise to large membrane vesicles containing accumulating amounts of mature, SEVs. This process suggests the capability of the viral glycoproteins to induce membrane fusion, and hence could explain the formation of large, pseudo-circular/pleomorphic membrane structures.

Nevertheless, Gn and Gc have been proven to have the capability of inducing membrane deformation, a phenomenon that may reflect the formation of a spherical-enveloped virus particle, as likewise proposed earlier for several other membrane enveloped (animal infecting) viruses (Kolesnikova *et al.*, 2004; Latham & Galarza, 2001; Shaw *et al.*, 2003). Transient expression of their glycoproteins gave rise to the formation of virus-like particles (VLPs). Some of the latter were shown to be pleomorphic in shape, not at all resembling mature virus particles, whereas in other cases VLPs were quite similar to authentic virus particles. Whether the pleomorphic membrane structures observed in this study indeed do represent TSWV VLPs, remains to be further analysed.

The ER arrest of Gc in the absence of Gn may be due to an improper folding and subsequent entrapment in the ER by interaction with one of the ER-resident chaperone proteins, as previously observed for Uukuniemi phlebovirus newly synthesized Gn and Gc glycoproteins (Veijola & Pettersson, 1999).

Our studies, furthermore, demonstrate that Gn suppresses ER arrest of Gc, most likely by heterodimerization, leading to a change in the spatial distribution of Gc from ER to ERES. Since these loci are the regions within the ER where the COPII-coated membranes and/or vesicles responsible for ER-to-Golgi transport are concentrated (Hanton *et al.*, 2006), our results suggest a COPII dependency of the glycoproteins during transport between these two organelles.

TSWV is unique in its property to multiply and form virus particles in both plant and animal (insect vector) cells. Hence, its virus assembly process bridges (and should be compatible with) these two distinct cell types. From this point of view, TSWV may prove to be an interesting tool to use to study and compare glycoprotein behaviour and cell sorting signals in relation to the endomembrane system between plant and animal cell systems.

ACKNOWLEDGEMENTS

REFERENCES

Andersson, A. M., Melin, L., Persson, R., Raschperger, E., Wikstrom, L. & Pettersson, R. F. (1997). Processing and membrane topology of the spike proteins G1 and G2 of Uukuniemi virus. *J Virol* **71**, 218–225. Medline

Barco, A. & Carrasco, L. (1995). Human virus protein, poliovirus protein 2bc, induces membrane proliferation and blocks the exocytic pathway in the yeast *Saccharomyces-cerevisiae*. *EMBO J* **14**, 3349–3364. Medline

Boevink, P., Oparka, K., Cruz, S. S., Martin, B., Betteridge, A. & Hawes, C. (1998). Stacks on tracks: the plant Golgi apparatus traffics on an actin/ER network. *Plant J* **15**, 441–447. Medline

Booth, T. F., Gould, E. A. & Nuttall, P. A. (1991). Structure and morphogenesis of dugbe virus (*Bunyaviridae*, Nairovirus) studied by immunogold electron-microscopy of ultrathin cryosections. *Virus Res* **21**, 199–212. Medline

Brandizzi, F., Snapp, E. L., Roberts, A. G., Lippincott-Schwartz, J. & Hawes, C. (2002). Membrane protein transport between the endoplasmic reticulum and the Golgi in tobacco leaves is energy dependent but cytoskeleton independent: evidence from selective photobleaching. *Plant Cell* **14**, 1293–1309. Medline

Carette, J. E., Stuiver, M., Van Lent, J., Wellink, J. & Van Kammen, A. B. (2000). Cowpea mosaic virus infection induces a massive proliferation of endoplasmic reticulum but not Golgi membranes and is dependent on de novo membrane synthesis. *J Virol* **74**, 6556–6563. Medline

Carette, J. E., van Lent, J., MacFarlane, S. A., Wellink, J. & van Kammen, A. (2002). Cowpea mosaic virus 32- and 60-kilodalton replication proteins target and change the morphology of endoplasmic reticulum membranes. *J Virol* **76**, 6293–6301. Medline

daSilva, L. L. P., Taylor, J. P., Hadlington, J. L., Hanton, S. L., Snowden, C. J., Fox, S. J., Foresti, O., Brandizzi, F. & Denecke, J. (2005). Receptor salvage from the prevacuolar compartment is essential for efficient vacuolar protein targeting. *Plant Cell* **17**, 132–148. Medline

Denecke, J. & Vitale, A. (1995). The use of plant protoplasts to study protein synthesis, quality control, protein modification and transport through the plant endomembrane system. *Methods Cell Biol* **50**, 335–348. Medline

Elliott, R. M. (1990). Molecular biology of the *Bunyaviridae*. *J Gen Virol* **71**, 501–522. Medline

Elliott, R. M. (1996). *The Bunyaviridae*. New York, NY: Plenum Press.

Gahmberg, N., Kuismanen, E., Keranen, S. & Pettersson, R. F. (1986). Uukuniemi virus glycoproteins accumulate in and cause morphological-changes of the Golgi-complex in the absence of virus maturation. *J Virol* **57**, 899–906. Medline

Goldbach, R. & Peters, D. (1996). Molecular and biological aspects of tospoviruses. In *The Bunyaviridae*, pp. 129–157. Edited by R. M. Elliott. New York, NY: Plenum Press.

Griffiths, G. & Rottier, P. (1992). Cell biology of viruses that assemble along the biosynthetic pathway. *Semin Cell Biol* **3**, 367–381. Medline

Hanton, S. L., Matheson, L. A. & Brandizzi, F. (2006). Seeking a way out: export of proteins from the plant endoplasmic reticulum. *Trends Plant Sci* **11**, 335–343. Medline

Haseloff, J., Siemering, K. R., Prasher, D. C. & Hodge, S. (1997). Removal of a cryptic intron and subcellular localization of green fluorescent protein are required to mark transgenic *Arabidopsis* plants brightly. *Proc Natl Acad Sci U S A* **94**, 2122–2127. Medline

Jantti, J., Hilden, P., Ronka, H., Makiranta, V., Keranen, S. & Kuismanen, E. (1997). Immunocytochemical analysis of Uukuniemi virus budding compartments: role of the intermediate compartment and the Golgi stack in virus maturation. *J Virol* **71**, 1162–1172. Medline

Karimi, M., Inze, D. & Depicker, A. (2002). GATEWAY™ vectors for *Agrobacterium*-mediated plant transformation. *Trends Plant Sci* **7**, 193–195. Medline

Kikkert, M., van Poelwijk, F., Storms, M., Kassies, W., Bloksma, H., van Lent, J., Kormelink, R. & Goldbach, R. (1997). A protoplast system for studying tomato spotted wilt virus infection. *J Gen Virol* **78**, 1755–1763. Medline

Kikkert, M., van Lent, J., Storms, M., Bodegom, P., Kormelink, R. & Goldbach, R. (1999). Tomato spotted wilt virus particle morphogenesis in plant cells. *J Virol* **73**, 2288–2297. Medline

Kikkert, M., Verschoor, A., Kormelink, R., Rottier, P. & Goldbach, R. (2001). Tomato spotted wilt virus glycoproteins exhibit trafficking and localization signals that are functional in mammalian cells. *J Virol* **75**, 1004–1012. Medline

Kitajima, E., de Avila, A. C., Resende, R., Goldbach, R. W. & Peters, D. (1992). Comparative cytological and immunogold labelling studies on different isolates of Tomato spotted wilt virus. *J Submicrosc Cytol Pathol* **24**, 1–14.

Kolesnikova, L., Berghofer, B., Bamberg, S. & Becker, S. (2004). Multivesicular bodies as a platform for formation of the Marburg virus envelope. *J Virol* **78**, 12277–12287. Medline

Kuismanen, E., Hedman, K., Saraste, J. & Pettersson, R. F. (1982). Uukuniemi virus maturation: accumulation of virus-particles and viral-antigens in the Golgi-complex. *Mol Cell Biol* **2**, 1444–1458. Medline

Latham, T. & Galarza, J. M. (2001). Formation of wild-type and chimeric influenza virus-like particles following simultaneous expression of only four structural proteins. *J Virol* **75**, 6154–6165. Medline

Lyons, M. J. & Heyduk, J. (1973). Aspects of developmental morphology of California encephalitis-virus in cultured vertebrate and arthropod cells and in mouse brain. *Virology* **54**, 37–52. Medline

Maliga, P., Sz-Breznovits, A. & Márton, L. (1973). Streptomycin-resistant plants from callus culture of haploid tobacco. *Nat New Biol* **244**, 29–30. Medline

Matsuoka, Y., Chen, S. Y., Holland, C. E. & Compans, R. W. (1996). Molecular determinants of Golgi retention in the Punta Toro G1 glycoprotein. *Arch Biochem Biophys* **336**, 184–189. Medline

Mohamed, N. A., Randles, J. W. & Francki, R. I. B. (1973). Protein composition of Tomato spotted wilt virus. *Virology* **56**, 12–21. Medline

Murashige, R. & Skoog, F. (1962). A revised medium for rapid growth and bioassays with tobacco tissue cultures. *Physiol Plant* **15**, 473–497.

Petterson, R. F. & Melin, L. (1996). Synthesis, assembly, and intracellular transport of *Bunyaviridae* membrane proteins. In *The Bunyaviridae*, pp. 159–188. Edited by R. M. Elliott. New York, NY: Plenum Press.

Rönnholm, R. (1992). Localization to the Golgi complex of Uukuniemi virus glycoproteins G1 and G2 expressed from clones cDNAs. *J Virol* **66**, 4525–4531. Medline

Rwambo, P. M., Shaw, M. K., Rurangirwa, F. R. & DeMartini, J. C. (1996). Ultrastructural studies on the replication and morphogenesis of Nairobi sheep disease virus, a Nairovirus. *Arch Virol* **141**, 1479–1492. Medline

Salanueva, I. J., Novoa, R. R., Cabezas, P., Lopez-Iglesias, C., Carrascosa, J. L., Elliott, R. M. & Risco, C. (2003). Polymorphism and structural maturation of Bunyamwera virus in Golgi and post-golgi compartments. *J Virol* **77**, 1368–1381. Medline

Shaw, K. L., Lindemann, D., Mulligan, M. J. & Goepfert, P. A. (2003). Foamy virus envelope glycoprotein is sufficient for particle budding and release. *J Virol* **77**, 2338–2348. Medline

Smith, J. F. & Pifat, D. Y. (1982). Morphogenesis of Sandfly fever viruses (*Bunyaviridae* family). *Virology* **121**, 61–81. Medline

Snippe, M., Willem Borst, J., Goldbach, R. & Kormelink, R. (2007). Tomato spotted wilt virus Gc and N proteins interact *in vivo*. *Virology* **357**, 115–123. Medline

Stefano, G., Renna, L., Chatre, L., Hanton, S. L., Moreau, P., Hawes, C. & Brandizzi, F. (2006). In tobacco leaf epidermal cells, the integrity of protein export from the endoplasmic reticulum and of ER export sites depends on active COPI machinery. *Plant J* **46**, 95–110. Medline

Veijola, J. & Pettersson, R. F. (1999). Transient association of calnexin and calreticulin with newly synthesized G1 and G2 glycoproteins of Uukuniemi virus (family *Bunyaviridae*). *J Virol* **73**, 6123–6127. Medline

Whitfield, A. E., Ullman, D. E. & German, T. L. (2005). Tospovirus-thrips interactions. *Annu Rev Phytopathol* **43**, 459–489. Medline

Wijkamp, I., van Lent, J., Kormelink, R., Goldbach, R. & Peters, D. (1993). Multiplication of tomato spotted wilt virus in its insect vector, *Frankliniella occidentalis. J Gen Virol* **74**, 341–349. Medline
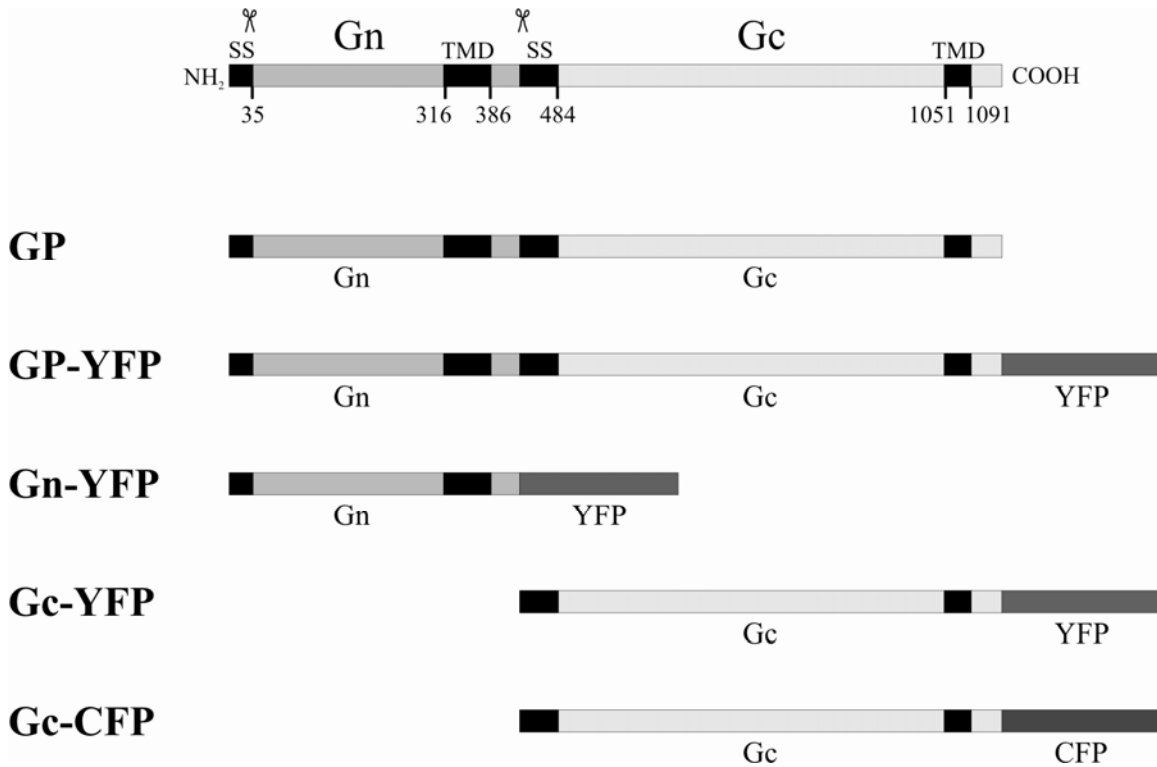
Fig. 1. Topology of the TSWV glycoprotein precursor. Constructs used for expression studies aligned below the precursor. Predicted cleavage sites (scissor symbols), hydrophobic areas (black boxes) and amino acid positions are indicated (SS, signal sequence; TMD, transmembrane domain). In all constructs, the YFP or CFP fluorophores were fused in-frame at the position of the stop codon.
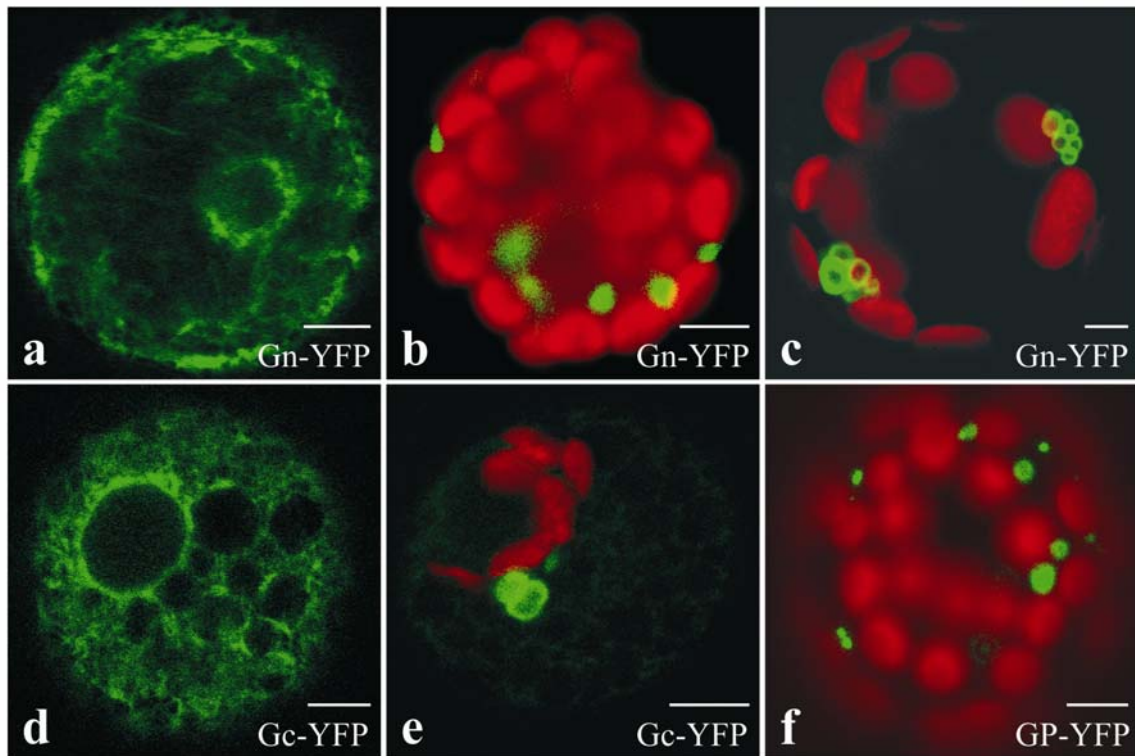
Fig. 2. Fluorescence images of *N. tabacum* protoplasts transfected with constructs coding for the TSWV glycoproteins. (a–c) Protoplasts transfected with Gn–YFP observed 24 h (a) and 48 h (b and c) p.t. (d and e) Protoplasts transfected with Gc–YFP observed at 48 h p.t. (f) Protoplast transfected with GP–YFP observed at 24 h p.t. The red fluorescing structures in (b), (c), (e) and (f) correspond to chloroplasts. Bars, 5 μm.
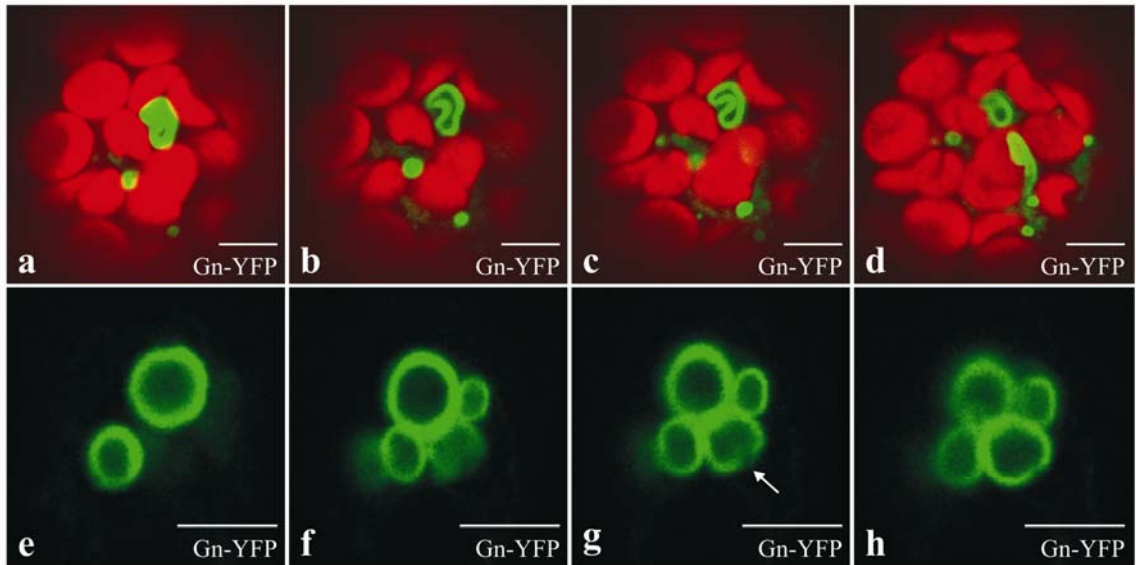
Fig. 3. Z-stack fluorescence images of *N. tabacum* protoplasts transfected with Gn–YFP. (a–d and e–h) Represent four sequential sections of two different protoplasts. An opening at one end of a pseudo-circular membrane structure is indicated by an arrow in (g). The red fluorescing structures in (a–d) correspond to chloroplasts. Bars, 5 μm.
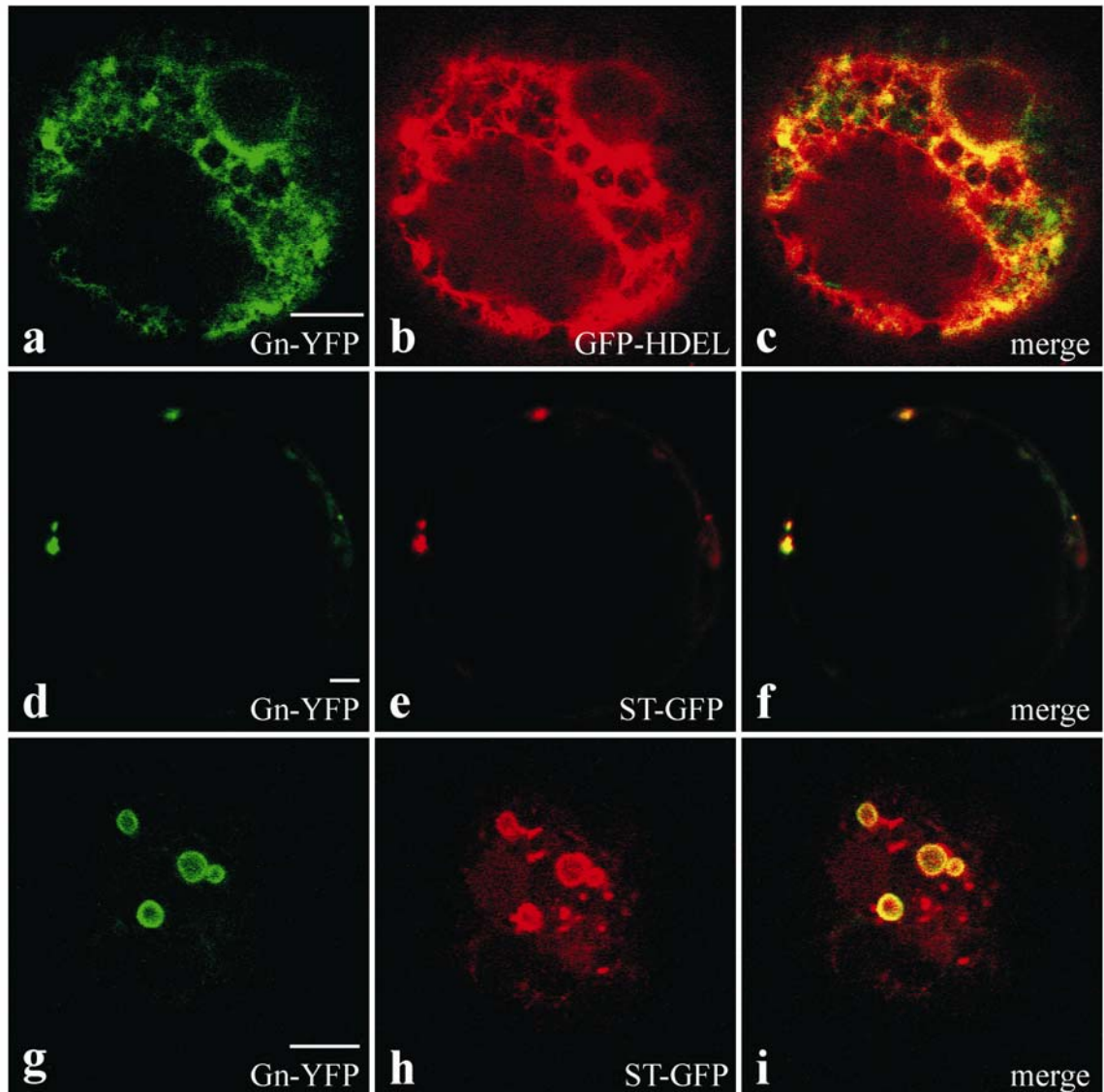
Fig. 4. Fluorescence images of *N. tabacum* protoplasts co-transfected with a construct coding for the Gn glycoprotein- and organelle-specific (ER or Golgi) marker. (a–c) Protoplast transfected with (a) Gn–YFP and (b) GFP–HDEL 24 h p.t. (c) Merged image of (a) and (b). (d–f) Protoplast isolated from plants stably transformed with ST–GFP and transfected with Gn–YFP 48 h p.t.: (d) Gn–YFP, (e) ST–GFP and (f) merged image of (d) and (e). (g–i) Protoplast isolated from plants stably transformed with ST–GFP and transfected with Gn–YFP 48 h p.t.: (g) Gn–YFP, (h) ST–GFP and (i) merged image of (g) and (h). Bars, 5 μm.
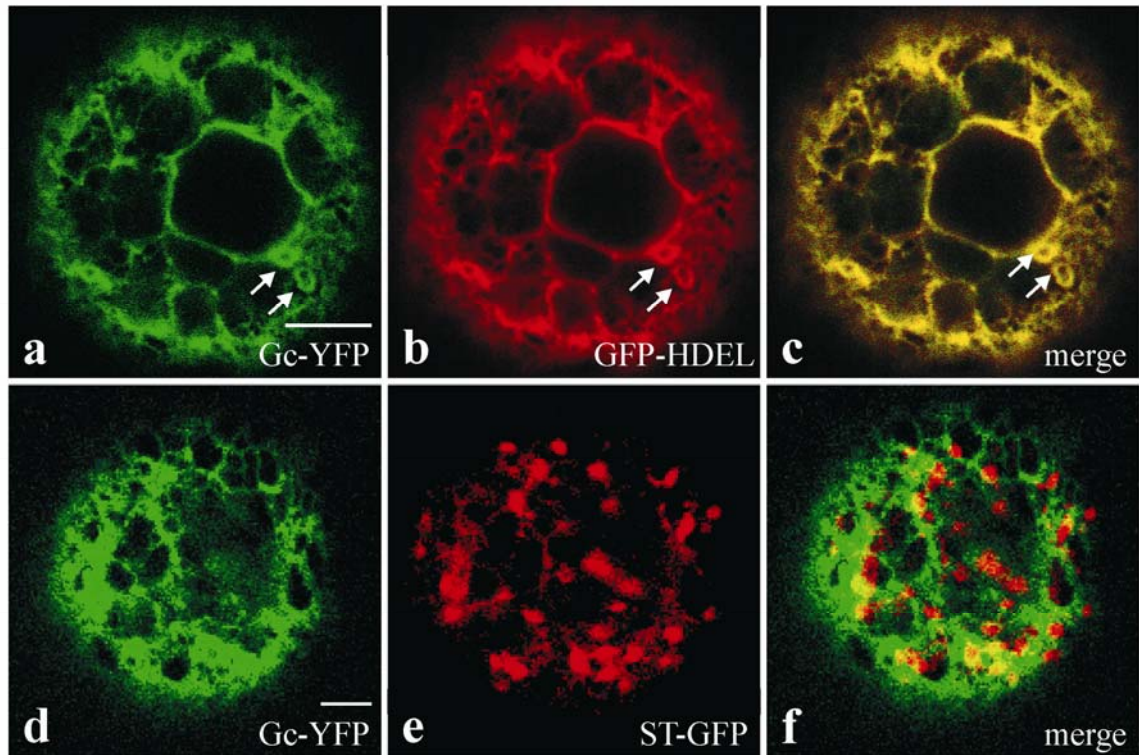
Fig. 5. Fluorescence images of *N. tabacum* protoplasts co-transfected with a construct coding for the Gc glycoprotein- and organelle-specific (ER or Golgi) marker. (a–c) Protoplast transfected with (a) Gc–YFP and (b) GFP–HDEL 24 h p.t. (c) Merged image of (a) and (b), arrows indicate pleomorphic structures. (d–f) Protoplast isolated from plants stably transformed with ST–GFP and transfected with Gc–YFP 24 h p.t.: (d) Gc–YFP, (e) ST–GFP and (f) merged image of (d) and (e). Bars, 5 μm.
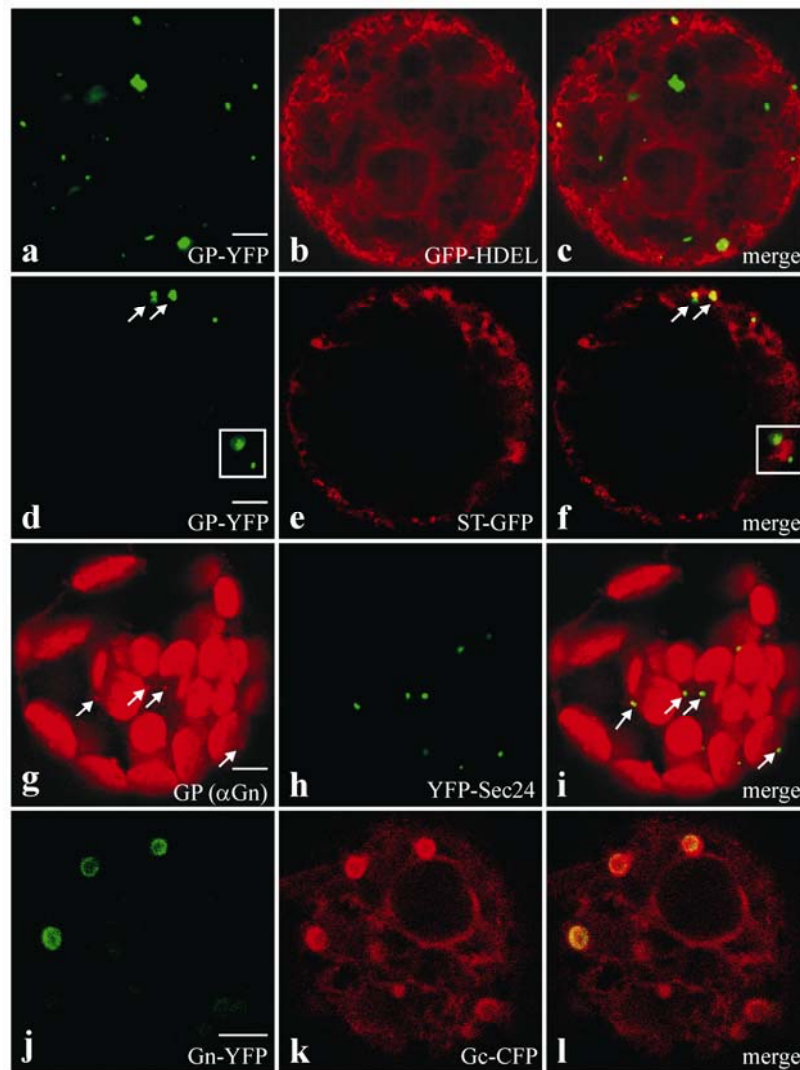
Fig. 6. Fluorescence images of *N. tabacum* protoplasts transfected with constructs coding for the glycoproteins Gn and Gc (from the common glycoprotein precursor or independent constructs) and organelle-specific (ER or Golgi) or ERES markers. (a–c) Protoplast transfected with (a) GP–YFP (Gc–YFP) and (b) GFP–HDEL 24h p.t. (c) Merged image of (a) and (b). (d–f) Protoplast isolated from plants stably transformed with ST–GFP and transfected with GP–YFP 24 h p.t.: (d) GP–YFP (Gc–YFP), (e) ST–GFP and (f) merged image of (d) and (e), arrows and squares indicate globular structures containing GP–YFP that co-localize and do not co-localize with ST–GFP, respectively. (g–i) Protoplast transfected with GP and YFP–Sec24 and immunolocalized with antibodies raised against Gc 24 h p.t.: (g) Gc (GP) indicated by arrows, (h) YFP–Sec24 and (i) merged image of (g) and (h) with co-localizations indicated by arrows. The large red fluorescing structures in (g) and (i) correspond to chloroplasts. (j–l) Protoplast transfected with (j) Gn–YFP and (k) Gc–CFP 24 h p.t. (l) Merged image of (j) and (k). Bars, 5 µm.
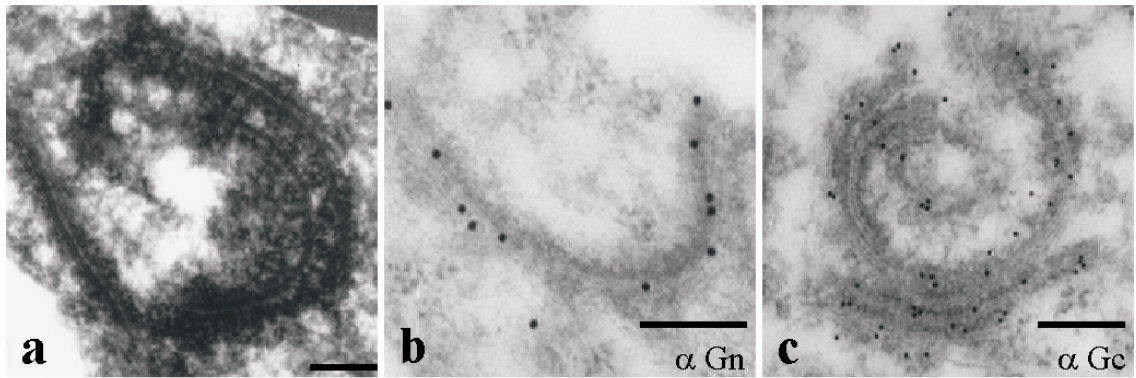
Fig. 7. Electronmicrograph showing dilated Golgi stacks and paired parallel membranes in TSWV-infected *Nicotiana rustica* plant cells [with permission from Kikkert *et al.* (1999)]. (a) Curved Golgi cisternae surrounding ribonucleocapsids; immuno-gold labelling analysis with antiserum against (b) Gn and (c) Gc. Bars, 200 nm.